International Journal of Hydrogen Energy 110 (2024) 371–385

Contents lists available at ScienceDirect

International Journal of Hydrogen Energy

journal homepage: www.elsevier.com/locate/he

Physics-informed data-driven Bayesian network for the risk analysis of hydrogen refueling stations

Jinduo Xing [a,*], Jiaqi Qian [a], Rui Peng [b], Enrico Zio [c,d]

[a] School of Mechanical-Electronic and Vehicle Engineering, Beijing University of Civil Engineering and Architecture, Beijing, 100044, China
[b] School of Economics and Management, Beijing University of Technology, Beijing, 100124, China
[c] MINES Paris-PSL University, CRC, Sophia Antipolis, France
[d] Energy Department, Politechnico di Milano, Milano, Italy

ARTICLE INFO

Handling Editor: Prof B Shabani

Keywords:
Hydrogen refueling stations
Risk analysis
Data-driven Bayesian network
CTGAN

ABSTRACT

The safety of hydrogen refueling stations (HRSs) is receiving increasing attention with the growth use of hydrogen energy. Existing risk assessment methods of HRS are primarily based on expert knowledge, which is affected by potential subjectivity. This paper aims to present a new hybrid risk assessment method incorporating HRS accident data and physical knowledge into a Bayesian network (BN) model to analyze the key risk influencing factors (RIFs). The HRS accident data in HIAD 2.1 from 1980 to 2023 is used in this paper, and 30 RIFs are identified based on the accident report information and physical knowledge. To address the issue of the insufficient accident data for BN modeling, the accident data is expanded by Conditional Tabular Generative Adversarial Networks (CTGAN). Bayesian search, Peter-Clark algorithm and Greedy Thick Thinning methods are adopted for structure learning. The expectation maximization algorithm is employed for parameter learning in the BN model. Additionally, K-fold cross validation is used when testing the performance of different BN models.

1. Introduction

With the growing demand for sustainable energy, hydrogen is receiving increasing attention. Sayem M. Abu et al. tuned a proportional-integral controller using a particle swarm optimization (PSO) algorithm to improve the stability and oxygen utilization of the system, as well as to reduce the dependence on the power grid [1]. In the case of fuel cell hybrid vehicles, Hyun Sung Lim et al. focused on improving the efficiency of hydrogen utilization by optimizing the energy management control strategy [2]. In addition, the usage of small fuel cells to provide emergency power for automation equipment is becoming feasible and intensifying, especially for remote areas or environments where power outages are prone to occur. B.V. Malozyomov et al. proposed a solution to provide power for automated control system equipment, further expanding the application areas of fuel cells [3].

As an indispensable part of the hydrogen energy infrastructure, urban hydrogen refueling stations (HRSs) play a key role in the decarbonization transition process of urban transport systems [4]. However, due to the characteristics of hydrogen, such as low minimum ignition energy, wide explosive limit and flammability range, and fast flame speed [5], HRS are exposed to multiple risk scenarios during operation. Without effective risk management, HRSs can lead to serious accidents, endangering the safety of people and environmental stability. For example, in May 2019, an explosion occurred at a hydrogen fuel storage tank located in South Korea, which resulted in two instant deaths and six injuries [6]. Therefore, it is particularly important to prevent multiple HRS accidents for ensuring operation safety [7]. For this, it is necessary to carry out risk analyses to discover the key risk-influencing factors.

Hydrogen production, storage, and transportation face numerous challenges. Currently, hydrogen production mostly relies on fossil fuels (gray hydrogen), which accounts for about 96% of global hydrogen production [8]. To advance the production of green hydrogen, the research by Hossain et al. focuses on solar energy for hydrogen production [9]. With advances in concentrated solar power (CSP) systems, the efficiency of solar thermal hydrogen production has reached 45%, much higher than that of conventional electrolysis methods. At this stage, storing hydrogen at low temperatures (−253 °C) or high pressures (700 bar) remains a significant challenge [10], both storage efficiency and safety need to be improved. Additionally, the efficiency of electrolysis technology still ranges from 60% to 80%, and production costs remain relative high [11].

Efforts have been devoted to investigating HRSs accidents for the identification of risk factors and failure processes by leveraging Fault

* Corresponding author.
E-mail address: xingjinduo@bucea.edu.cn (J. Xing).

https://doi.org/10.1016/j.ijhydene.2025.02.110
Received 5 December 2024; Received in revised form 28 January 2025; Accepted 6 February 2025
Available online 20 February 2025

Acronyms

BN	Bayesian network
BS	Bayesian search
CPT	Conditional probability table
CTGAN	Conditional Tabular Generative Adversarial Network
DAG	Directed acyclic graph
DBN	Dynamic Bayesian Network
EM	Expectation Maximization Algorithm
FTA	Fault tree analysis
GAN	Generative Adversarial Network
GTT	Greedy Thick Thinning
HRSs	Hydrogen refueling stations
HIAD	Hydrogen Incidents and Accidents Database
MLE	Maximum likelihood estimation
OA	Overall accuracy
PC	Peter-Clark Algorithm
RIFs	Risk-influencing factors

Symbols

$Pa\ (A_i)$	The parent node of variable A_i in BN
$cov(X, Y)$	The covariance of X and Y
σ_X	The standard deviation of X
σ_Y	The standard deviation of Y
I_P	The information of the condition variable
x_{ii}	The ith state of the attribute variable X_i
x_{ji}	The ith state of the attribute variable X_j
C_i	The ith state of the attribute variable C
$\theta^{(t)}$	The current parameter
$Q\ (\theta\mid \theta^{(t)})$	The expected value of the hidden variable Z under the current $\theta(t)$
$P\ (Z, X\mid\theta^{(t)})$	The posterior probability distribution of the hidden variable Z
$\theta^{(t+1)}$	The updated model parameters in the t+1st iteration

Tree Analysis (FTA) [12], Bow-tie (BT) [13] and Bayesian Networks (BN) [14], Systems theoretic accident model and process (STAMP) [15] methods. For instance, Li et al. conducted dynamic risk assessment of HRS by integrating Dynamic Bayesian Networks (DBN) with Markov chains [16]. Wu et al. proposed a whole-process hydrogen accident risk assessment model to prevent accidents and control the corresponding risk [17]. Alternatively, He et al. developed a comprehensive resilience assessment framework for HRS [18].

In previous studies on HRS risk identification, researchers have also focused on HRS accident consequence simulation. Lin et al. analyzed the dispersion characteristics of hydrogen storage tanks after leakage under different wind conditions by using FLUENT [19]. Yang et al. constructed a risk analysis model of BN, which reveals the main factors affecting maritime safety [20]. Zhang et al. proposed a physics-informed graph neural network for the modeling and predicting of hydrogen jet and diffusion [21].

Existing methods for risk assessment of hydrogen refueling stations are mainly based on expert knowledge to model failure processes [22]. This manually-designed structure is likely to be subjective, leading to a lack of accuracy. Inadequate data is another challenge for implementing a data-driven method. Regarding the study of HRS accidents, historical data is usually insufficient. To deal with the issue of data deficiency, this paper builds a physical-data-driven model by incorporating the HRS accident data and physical knowledge into a BN model, combining the physical model with a data-driven approach.

Hydrogen Incidents and Accidents Database (HIAD 2.1) is the most authoritative on hydrogen accidents. It includes the updating of more than a thousand hydrogen accidents worldwide (as of September 2023), but only 104 accidents are related to HRSs. To address the problem of few data, in this paper we use Generative Adversarial Network (GAN) to augment the data size.

The core concept of GAN is to generate data through an adversarial process that involves two models: a Generator and a Discriminator. Initially, GAN was mainly applied to image synthesis [23], art creation, drug discovery [24]. One of the advantages of GAN is that it does not require labelled data for training [25]. In these fields, data is often protected by privacy regulations, making it difficult to obtain. Both GANs and Conditional Tabular Generative Adversarial Network (CTGANs) can generate high-quality synthetic data, which can be used to train risk assessment models, thereby addressing issues of data imbalance or missing data. In the foreign exchange market, Kexin Peng and others used GANs to predict exchange rate returns. The optimized GAN model, through the Nash equilibrium, handled the nonlinear relationships in exchange market data, effectively improving trading decisions and risk assessment capabilities [26]. Biao He and others used CTGANs to generate synthetic over-sampling datasets, increasing the diversity and quantity of data. Research has shown that the synthetic datasets generated by CTGANs can retain the characteristics of real data, addressing issues of data shortage and imbalance, and providing reliable support for risk management in tunnel blasting engineering [27]. Kang Zhang and others used CTGANs to simulate and predict stock market risks, helping investors assess risk exposure under different investment strategies. CTGANs are able to learn price patterns from historical stock market data and generate similar predictive data [28].

Physical-data-driven methods have made progress in several areas in recent years. You Wang et al. fused the Chaotic Adaptive Sparrow Search Algorithm (CASSA) with physical information to improve prediction accuracy and demonstrated strong stability and generalization ability in data prediction across various scales [29]. Qin Li et al. combined physical models with deep learning to improve the estimation accuracy of vehicle dynamic states [30]. Meng et al. constructed data-driven BN for blowout and lithium-ion battery accidents by integrating expert knowledge and accident data [31,32]. Tobias Glück et al. proposed a combination of physical modeling and a data-driven approach to improve the estimation accuracy of vehicle dynamic states. Additionally, Tobias Glück et al. proposed a hybrid control strategy that combines physical modeling with a data-driven approach to approximate the nonlinear behavior of the system through a data-driven agent model, which exhibited accelerated results during the commissioning of a new valve model [33]. This approach provides a new solution for the precise control of hydraulic systems.

Leveraging all the above, in this work, a physics-informed data-driven BN modeling approach by HRS risk analysis is developed. The main contributions can be summarized as follows:

(1) Develop a new physics-informed data-driven risk assessment method for HRSs.
(2) Use of the CTGAN method for addressing the issue of limited accident data.
(3) Identification of risk factors for HRS.

The remaining of the paper are organized as following. The proposed methodology is presented in Section 2. In Section 3, the data collectiong and processing processes are dedicated. Section 4 performs a case study to verify the effectiveness of the proposed method. Finally, Section 5 concludes the work.

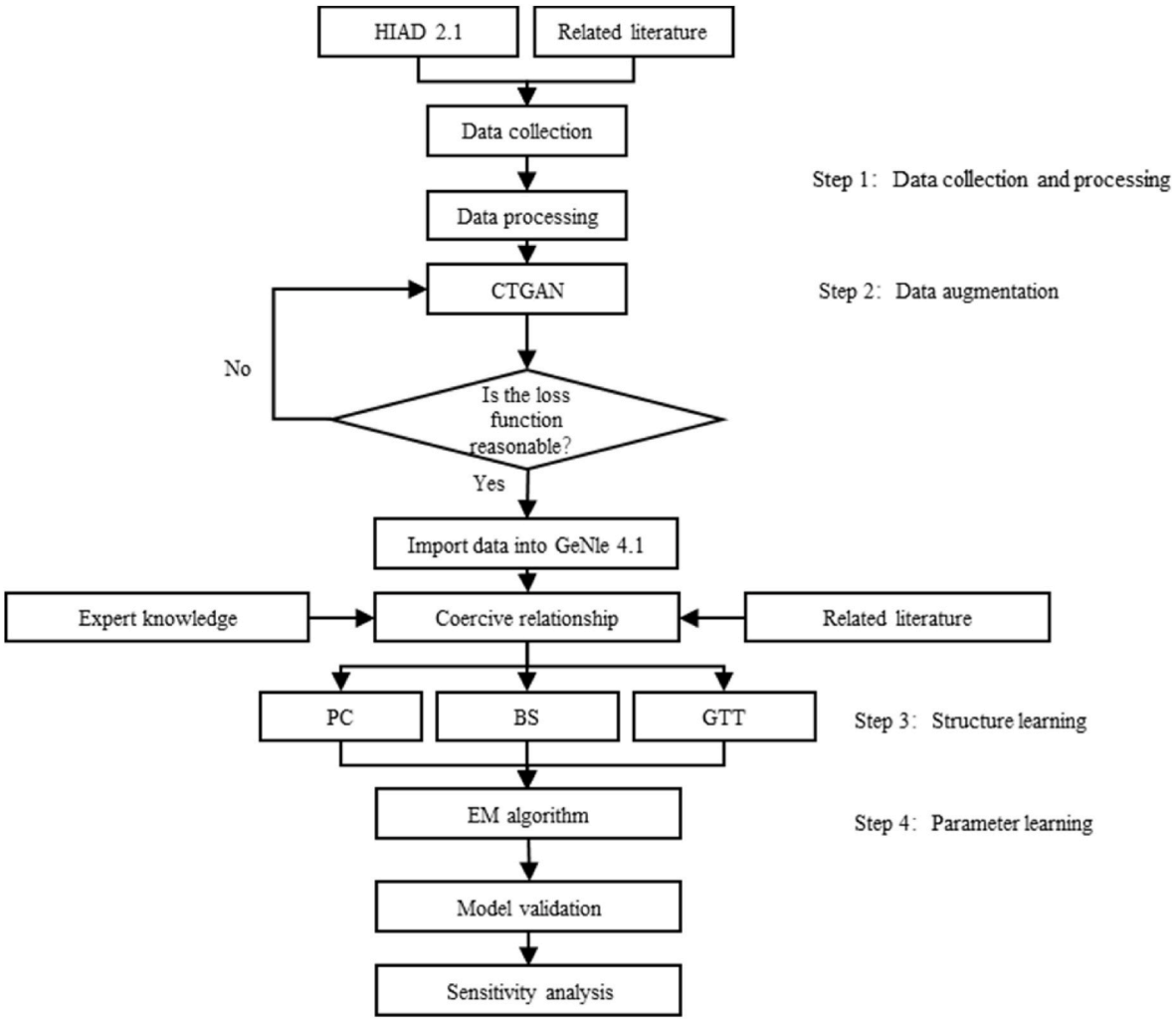

Fig. 1. Framework of physics-informed data-driven HRS risk analysis.

2. Methodology

2.1. Method framework

The basic structure of this work is shown in Fig. 1. First, the accident data on HRS refers to a set of accident investigation reports. The collected data can be processed and merged in to table form to support the following model construction process. Due to the limited data size, CTGAN method is applied to augment the data. Then, the augmented data can be fed into BN to conduct structure learning and parameter learning. Specifically, PC, BS and GTT are employed for structure learning. Additionally, EM algorithm is used for parameter learning. K-fold cross-validation is conducted to compare the performance of the above three BN models. Through sensitivity analysis, the importance of each RIF is determined, laying the foundation for subsequent risk management.

2.2. Bayesian Networks

BN is a graphical network based on probabilistic reasoning [34], which is a combination of probability theory and graph theory. The topology of a BN is a directed acyclic graph, where the nodes represent random variables, which can be observable variables or hidden variables, unknown parameters, etc. The fundamentals of BN are given in formula (1) and (2) [35]. By considering the conditional dependencies of n random variables A_1, A_2, …, A_n, a directed acyclic graph with n nodes depicts the joint probability $P(U)$ of variables $U = \{A_1, A_2, \ldots, A_n\}$ [7].

$$P(U) = \prod_{i=1}^{n} P(A_i|P_a(A_i)) \tag{1}$$

where $Pa\ (Ai)$ denotes the parent node of variable A_i in BN.

Based on BN's theorem, given new observation or evidence E, BN can update the prior probabilities of variables with rendering posterior probabilities [17].

$$P(U|E) = \frac{P(E|U)P(U)}{P(E)} = \frac{P(U,E)}{\sum_U P(U,E)} \tag{2}$$

3. Data collection and processing

3.1. Data collection and pre-processing

The initial data for this study was obtained from the HIAD 2.1 database [36], which is a hydrogen database that is continually being updated to provide clearer descriptions of accidents, as well as casualties, lessons learned, and remedies. This database has a wide range of data sources that are covered globally. We gathered accident data from 1980 to September 2023 from it. To preclude the redundancy of generalized data, this study exclusively references a singular database.

Not only hydrogen accidents related to HRSs, but the other chemical accident related to hydrogen is included in HIAD 2.1. For example, hydrogen explosions in certain chemical plants are often caused by

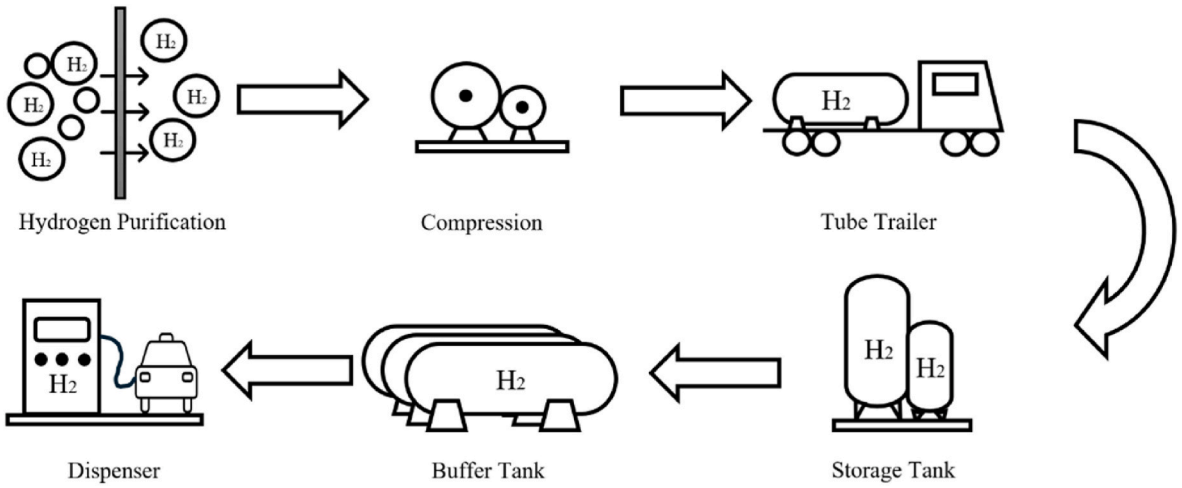

Fig. 2. HRS workflow diagram.

Table 1
Initial organized RIFs.

Symbol	Event	Symbol	Event
X1	Lack of risk assessment	X2	Unreasonable hot work procedures
X3	No fire arrester installed on the vent tube	X4	Electrical short circuit or overload
X5	Unqualified electrical piping material	X6	Abnormal heating of hydrogen due to throttling effect
X7	Unreasonable system (design, construction, installation or testing)	X8	Human-carried fire sources
X9	Ineffective management of flammable substances	X10	Lack of inspection or maintenance management
X11	Improper site selection	X12	Vehicle collision
X13	Natural disaster	X14	Third party influence
X15	Delayed medical care	X16	Fractured hose connection
X17	Emergency drills not conducted or ineffective	X18	Seal failure at pipe joints
X19	Hydrogen embrittlement occurs	X20	Weld cracking
X21	No emergency plan or unreasonable preparation	X22	Compressor seal failure
X23	Uneven flange preload	X24	Insufficient screw torque of value
X25	Lack of training or experience	X26	Poor organizational system
X27	Unreasonable regulations	X28	Ambient hydrogen detection device failure
X29	Malfunction of pressure detection device	X30	Unreasonable detection range or layout
X31	Sensor failure	X32	Manual emergencies stop system failure
X33	No emergency awareness or delay response	X34	Not following emergency procedure
X35	PLC failure	X36	Solenoid value failure
X37	Automatic sprinkler system failure	X38	Not wearing electrostatic protective clothing, shoes and hats
X39	Improper operation	X40	Fire detection device malfunction
X41	Failure of pressure relief device	X42	No electrostatic protective equipment
X43	Lack of attention to aging and rusting	X44	Mechanical collision produces sparks
X45	Pressure regulator fault	X46	Unreasonable cable laying
X47	Filter failure	X48	Impure hydrogen
X49	High gas flow due to compressor degradation	X50	No foreign object blocking device is installed in the release tube
X51	Insufficient pressure resistance of materials		

improper storage or reactor failure. During hydro processing, reactors can explode due to equipment failure causing accidental contact with hydrogen with other reactants. In chemistry laboratories, explosions can be caused by inadvertent mixing of hydrogen with strong oxidizing agents such as chlorine. The initial step involved the extraction of hydrogen accidents associated with HRS from the HIAD 2.1. Subsequently, through the meticulous sorting and categorization of these incidents, coupled with a comprehensive review of extant literature, it was ascertained that leakage, fire, and explosion are the predominant types of accidents associated with HRS [17].

Leakage refers to the accidental escape of hydrogen from storage, transportation, or use equipment, leading to an increase in the hydrogen concentration in the air, which raises the risk of fire and explosion. Fire occurs when hydrogen gas, mixed with air, combusts in the presence of an ignition source, potentially releasing heat and posing dangers to the surrounding environment. Explosion, on the other hand, is a violent reaction triggered by an external ignition source or other stimuli when the hydrogen-air mixture reaches its explosive limits in an enclosed or confined space, resulting in a strong shockwave and instantaneous release of energy. These hazards highlight the critical importance of safety measures when working with hydrogen.

As shown in Fig. 2, the process flow of HRS involves multiple stages of hydrogen purification, compression, transport, storage, buffering and refueling. After the initial data screening, 104 accidents that occurred within the working area of the HRS were screened from HIAD 2.1. It can be noted that most of the hydrogen accidents included in HIAD 2.1 occurred in chemical, pharmaceutical, refinery, silicon, and ammonia plants, where hydrogen is a by-product, and such accidents were excluded from the analysis [37].

In this study, we sorted and classified the RIFs for hydrogenation station accidents in the previous literature and then consolidated them to get 60 RIFs. The descriptive analyses in the complete description of the accident in HIAD 2.1 were disassembled, and one by one, they corresponded to the 60 RIFs derived from the above collation. We found that not all the RIFs have correspondences in the event descriptions, and categorized three RIFs that do not appear in prior knowledge: Lack of risk assessment, Unreasonable system (design, construction, installation or testing), and Lack of inspection or maintenance management. After collation, there are now 51 RIFs, as shown in Table 1.

We found that certain nodes had fewer occurrences, and less frequent occurrences may lead to insufficient influence of these nodes in the model, thus affecting the overall structure learning. Therefore, to improve the accuracy of the subsequent structure learning, it is necessary to merge these nodes to reduce noise and enhance the stability of the model. By merging the nodes, a more focused representation of the

Table 2
RIFs for HRS accidents.

Symbol	Event	Symbol	Event
X1	Unexpected source of ignition	X2	Inadequate maintenance
X3	Vehicle collision	X4	Uneven flange preload
X5	Insufficient screw torque value	X6	Non-compliance with emergency procedures
X7	Mishandling	X8	Lack of risk assessment
X9	Poor system design	X10	Lack of training or experience
X11	Inadequate organizational systems	X12	Unreasonable provisions
X13	Emergency management deficiencies	X14	Pipe joint seal failure
X15	Failure of environmental hydrogen detection device	X16	Failure of pressure detection device
X17	Unreasonable detection range or layout	X18	Failure of the emergency response system
X19	Electromagnetic threshold fault (physics)	X20	Pressure relief device failure
X21	Filter failure	X22	Electrical short circuit or overload
X23	Hose fitting rupture	X24	Hydrogen embrittlement
X25	Weld cracking	X26	Inadequate material performance
X27	Abnormal heating of hydrogen due to throttling effect	X28	Natural disaster
X29	Third-party impact	X30	Radioactive isotope of hydrogen

dataset can be made, which helps to extract more effective features and relationships, thus optimizing the learning process. Ultimately, this strategy can help to improve the performance and generalization of the model in subsequent learning tasks [38].

Specifically, it lies in grouping nodes with similar features into one category to avoid affecting the overall learning effect because individual nodes appear too infrequently. For example, in the case of fire source-related events, we merge the nodes related to accidental fire sources. Specifically, nodes X8 (Human-carried fire sources), X38 (Not wearing electrostatic protective clothing, shoes and hats), X42 (No electrostatic protective equipment), and X44 (Mechanical collision produces sparks) are all related to the formation and propagation of fire sources, and thus they are considered as the same class of events. Although the specific manifestations of these events are different, they all belong to the potential ignition sources that start fires and merging them can help the model more accurately identify the occurrence pattern of ignition sources.

Similarly, merging was performed in the nodes related to irrational system design. Nodes X3(No fire arrester installed on the vent tube), X7 (Unreasonable system), X46 (Unreasonable cable laying), and X50 (No foreign object blocking device installed in the release tube) are nodes related to system design flaws and safety hazards. Although they describe different types of design irrationality respectively, fundamentally, they all belong to the category of improper system design or insufficient security protection, and merging these nodes helps the model to better understand the risks associated with design flaws.

Through this node merging approach based on the nature of events, we can simplify the data structure and reduce the noise while retaining the key safety hazard information, thus making the subsequent structural learning more efficient and precise. This merging not only helps to improve the generalization ability of the model but also makes the learning process better able to capture potential relationships between events. After this series of adjustments and integration, we finally obtained 30 new RIFs, as show in Table 2.

These new RIFs more centrally reflect the characteristics of various potential risks and cover different types of events and factors, making subsequent analysis and research more efficient. This reintegrated approach ensures a clearer representation of risk factors in subsequent structural studies, thus providing a more reliable basis for decision-making.

3.2. Data augmentation

Constructing reliable models using parametric learning faces considerable challenges due to the limited nature of available data. Insufficient data samples may lead to overfitting of the model during training, thus affecting its generalization ability and prediction accuracy. In this case, data augmentation techniques are particularly important and valuable [39]. Data augmentation not only effectively scales the training set but also improves the model's adaptability in different scenarios.

GAN is a deep learning model consisting of two neural networks: a Generator and a Discriminator [40]. These two networks are trained in an adversarial way to form a dynamic game process. It receives both real and generated samples and outputs a probability value indicating the likelihood that the input sample is real. The goal of the discriminator is to identify real and fake data as accurately as possible, thus minimizing its classification error rate.

During the training process, the generator and the discriminator are updated by alternating optimization. Specifically, the parameters of the discriminator are first fixed, and the generator is trained to produce higher quality samples; then the parameters of the generator are fixed, and the discriminator is trained to improve its recognition ability [41]. This adversarial training mechanism allows the generator to continuously improve the data it generates, capture the complex distributional features of the data, and ultimately generate highly realistic samples.

In this context, CTGAN, as an advanced generative model, can effectively compensate for the missing data. CTGAN generates new data samples with real features by learning the distribution of existing data. These generated data can be combined with the original data to form a more diverse training set [42].

To develop a data-driven BN model, the size of the dataset needs to be further extended to enhance the model's expressive capability. To this end, in this paper, a synthetic dataset containing 1180 samples is generated using CTGAN. This new synthetic dataset not only greatly enriches the original data in terms of quantity but also maintains consistency with the real data in terms of feature distribution, making the generated data more representative and effective. This process allows us to utilize a larger dataset to train the BN model and improve the prediction accuracy and robustness of the model in the case of data scarcity [43].

After extending data size, assessing the quality of the generated data is a crucial step. This process not only ensures that the generated data has practical application value but also improves the effectiveness of subsequent model construction. Therefore, it is necessary to choose an appropriate method to comprehensively assess the data generated. First, the quality of the synthetic dataset can be assessed by comparing the absolute difference in Pearson correlation coefficients (ρ) between the real and synthetic datasets, as shown in formula (3) [44]:

$$\rho_{X,Y} = \frac{cov(X, Y)}{\sigma_X \sigma_Y} \tag{3}$$

where $cov\ (X, Y)$ denotes the covariance of X and Y, and σ_X and σ_Y represents the standard deviation of X and Y, respectively. If the result is close to 1 or -1, it means that the linear relationship between the generated data and the real data is strong, indicating that the data generated by the GAN is somehow successful in capturing the features of the real data.

Second, subjective assessment is equally important. The expert review can judge the quality of the generated data by judging the loss function of the generator and discriminator that generate the data to ensure that the generated data meets the practical application requirements. In GAN training, the generator and discriminator are usually in a state of dynamic equilibrium [31]: as training proceeds, the

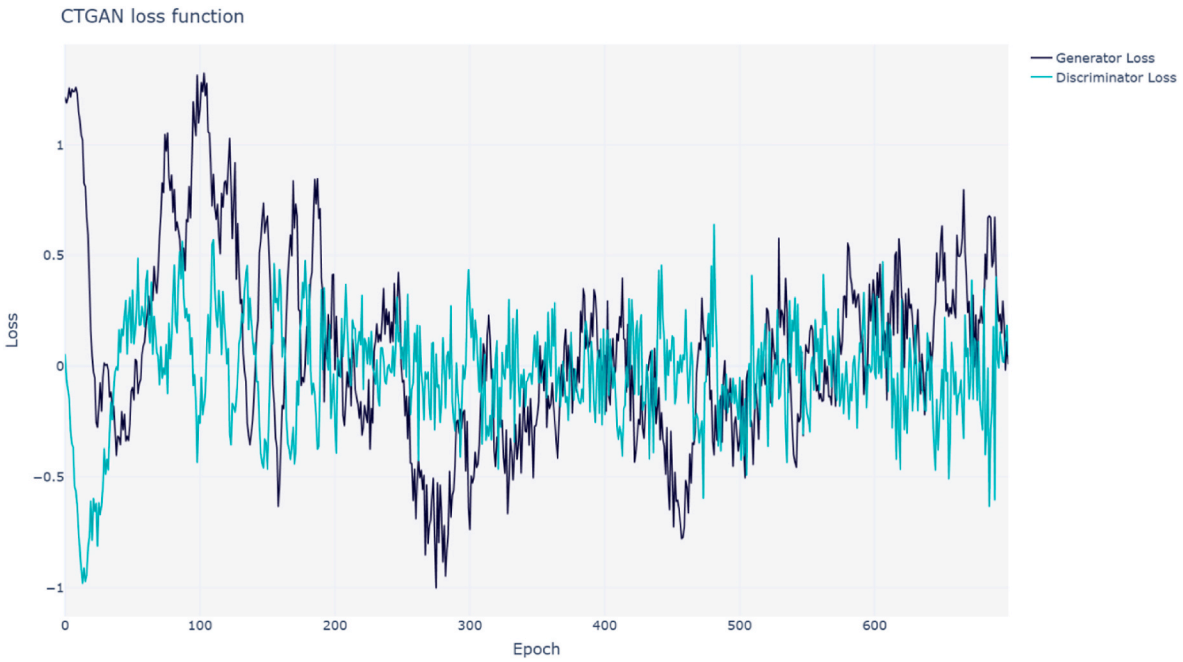

Fig. 3. CTGAN loss function.

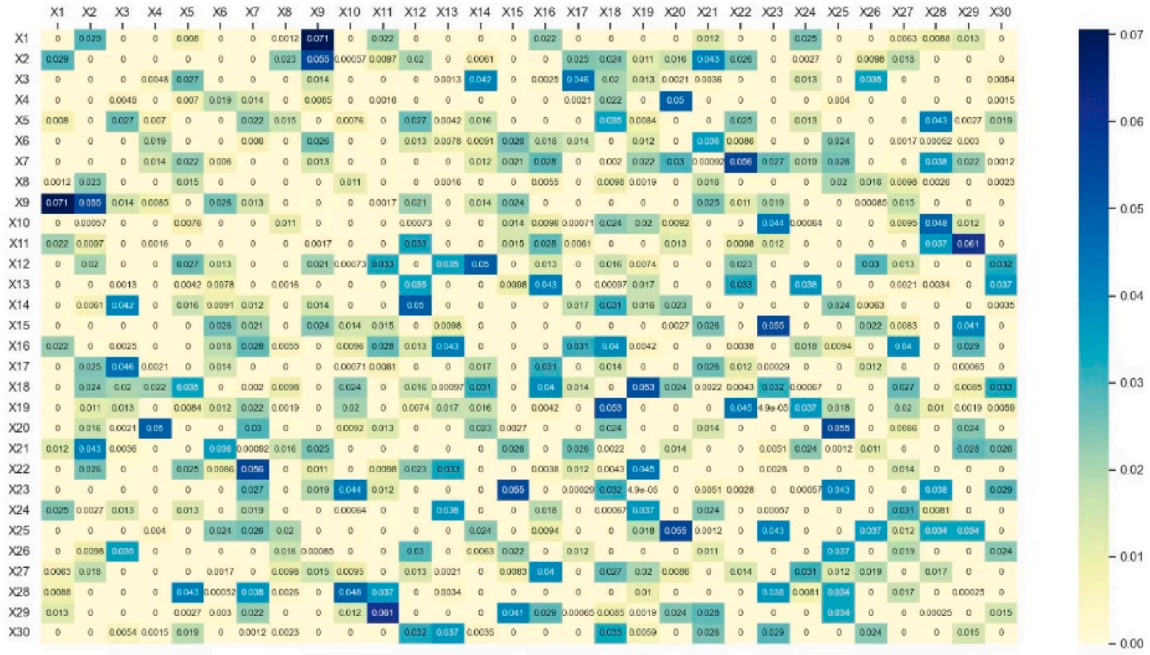

Fig. 4. Node strength and weakness relationship diagram.

generator need to gradually learn to generate more realistic data, and the loss need to gradually decrease. The discriminator's loss needs to be optimized with training. The loss curves of the two need to tend to be in equilibrium, as shown in Fig. 3, which plots the loss functions of the generator and the discriminator.

After completing the data evaluation, those generated data with good performance can be selected based on the evaluation results as the basis for subsequent model building. This step is critical to the performance of the model, and data quality can directly affect the accuracy and robustness of the model [45]. When selecting data with good results, consideration can be given to combining the results of multiple assessment methods to ensure that the selected data meets high standards in terms of quality and diversity.

Subsequently, we used the generated data to map the strengths and weaknesses of the nodes. We utilize conditional mutual information between attributes to construct a structure that accounts for the degree of interdependence of each node in the model, defined by formula (4) [46]:

$$I_P(X_i, X_j|C) = \sum_{x_{ii}, x_{ji}, C_i} P(x_{ii}, x_{ji}, C_i) log \frac{P(x_{ii}, x_{ji}|C_i)}{P(x_{ii}|C_i)P(x_{ji}|C_i)} \quad (4)$$

where I_P denotes the information of the condition variable, x_{ii} is the ith state of the attribute variable X_i, x_{ji} is the ith state of the attribute

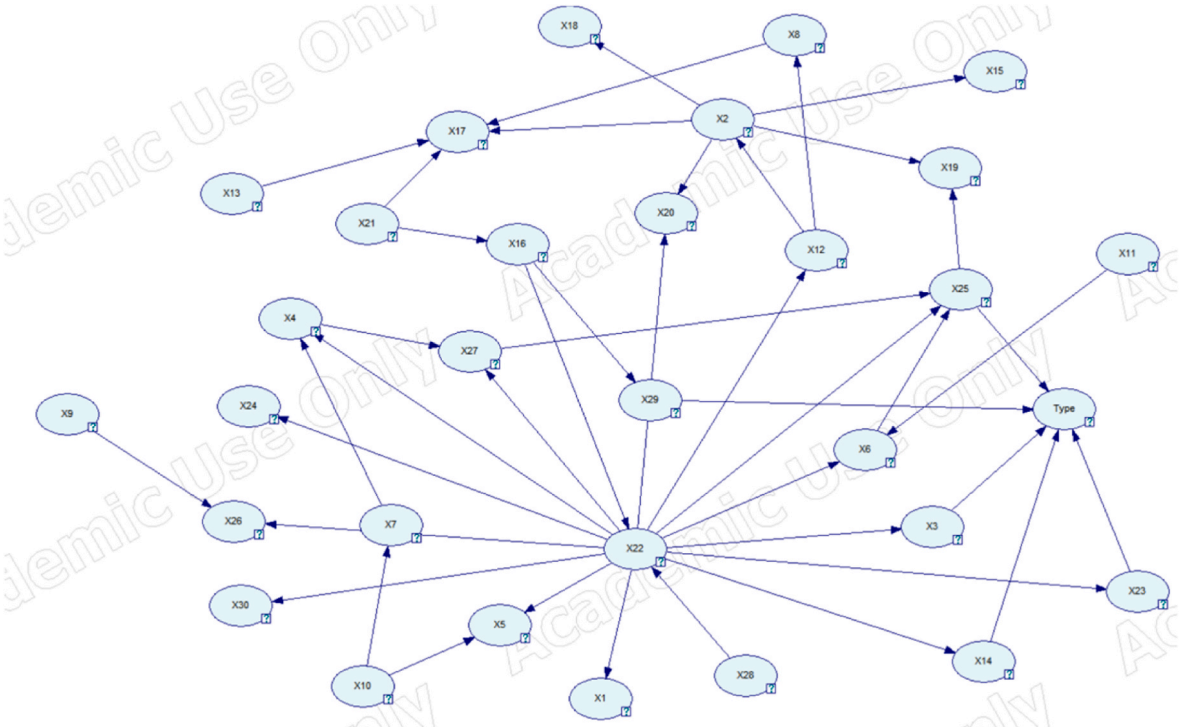

Fig. 5. Structure learning developed by BS algorithm.

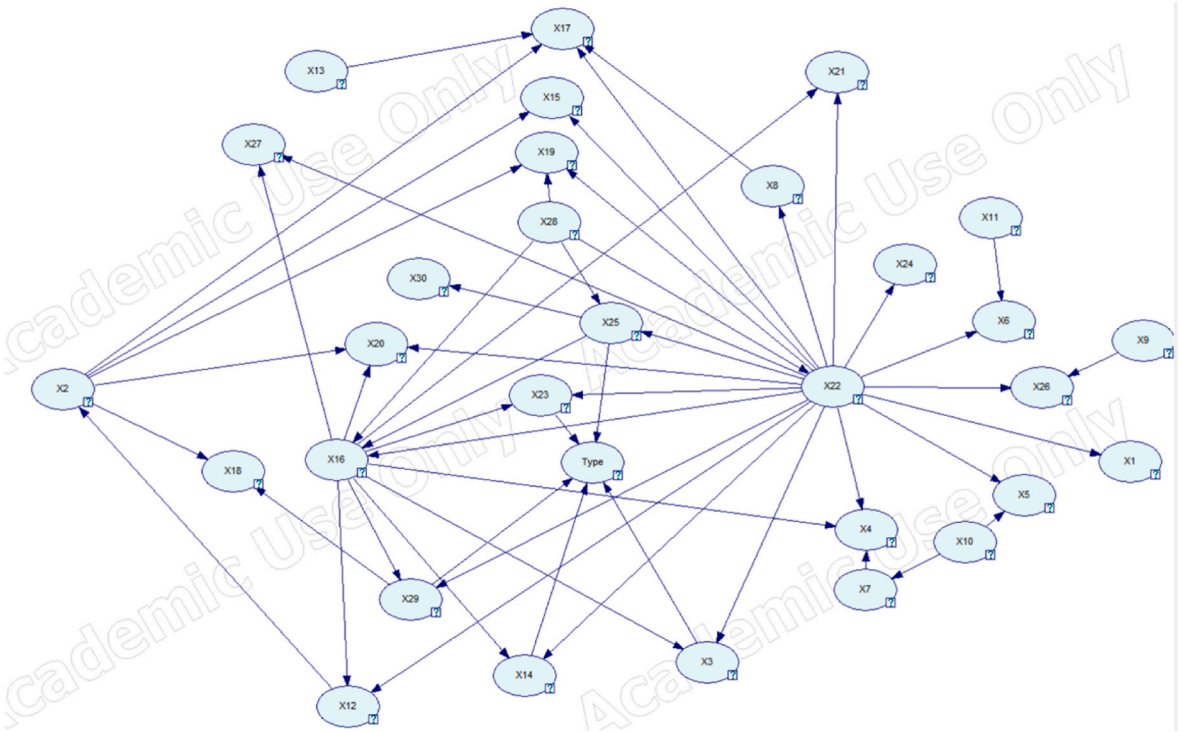

Fig. 6. Structure learning developed by GTT algorithm.

variable X_j, and C_i is the ith state of the attribute variable C.

As shown in Fig. 4, the degree of interaction and correlation between different nodes can be seen. The correlation values between the nodes range from a minimum of 0 to a maximum of 0.07, reflecting the strength of the relationship between them. Specifically, nodes with a correlation of 0.07 represent a very strong connection between them, while nodes with a correlation of 0 indicate that there is hardly any connection between them. By analyzing these strong and weak relationships, we can explore the characteristics of the nodes and their role in the overall system in greater depth.

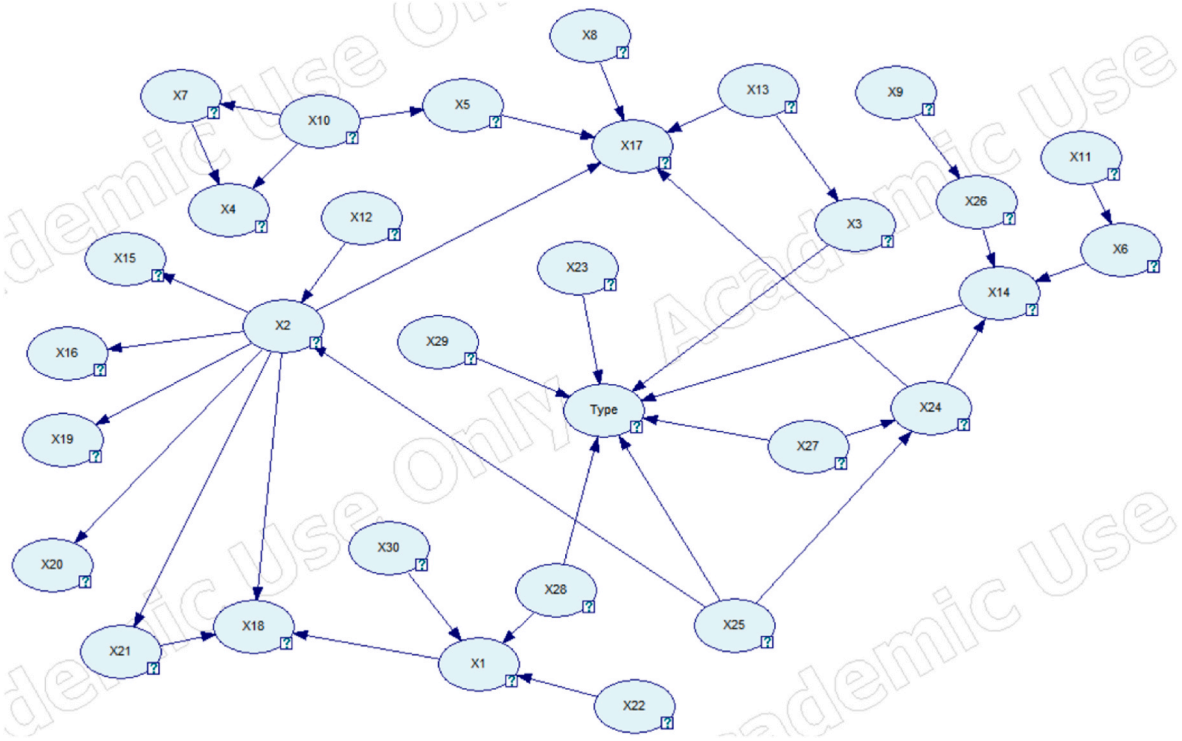

Fig. 7. Structure learning developed by PC algorithm.

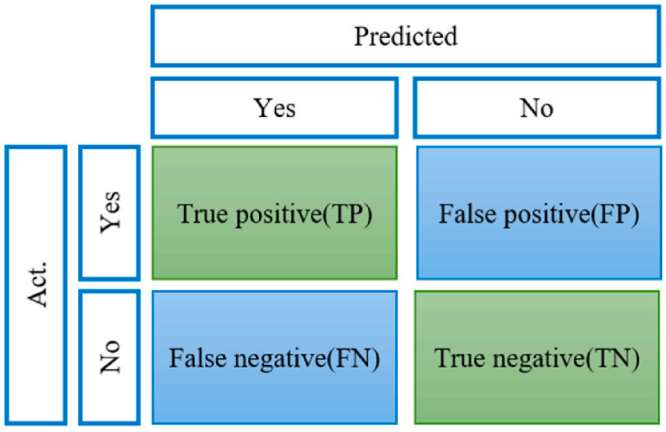

Fig. 8. Confusion matrix schematic.

Table 3
Predictive performance metrics of the three algorithms.

	OA	Precision	Recall	F_1 score
BS	91.8%	96.3%	99.4%	95.1%
GTT	90.2%	96.4%	86.4%	92.7%
PC	89.2%	89.4%	97.8%	93.8%

4. Case study

4.1. BN structure learning

Structure learning is the process of identifying and determining relationships between variables and their overall structure in a model with the goal of discovering a directed acyclic graph structure. In traditional BN, the network structure is usually designed manually by an expert based on prior knowledge. However, in complex network structures, the manually designed structure is likely to be subjective. It may lead to inaccurate inference when missing data is encountered. Data may be difficult to obtain in real situations. The Bayesian model of accident risk of hydrogen refueling stations developed in this paper suffers from the problem of insufficient data. In this paper, a physical model is combined with a data-driven approach to form a physical-data-driven model that can deal with uncertainty. The HRSs system is a complex multilevel and multifactor system with uncertainties, such as equipment failures, fluctuations in energy supply, and changes in the external environment. BN can handle these uncertainties and provide feasible decision support based on data-driven reasoning.

This study adopts a physics-informed and data-driven approach to structure learning with GeNIe 5.0 as a means of automatically identifying relationships and dependency structures between variables. Above all previous literature and experts' knowledge are organized to obtain background information and theoretical support to help identify possible causal relationships. In hydrogen refueling stations, there exists a lot of prior knowledge that can be fed into the network in advance. For example, the collision (friction) of metal objects can cause sparks, and fires can be caused within a certain hydrogen concentration range. Thus, an edge can be added in the two nodes of BN in advance. In this section, the processed data information is first input into the system, and then the physical information is used as an additional input to define the coercive relationship between different nodes.

Fig. 5 shows the HRS accident network model developed by the BS algorithm. In the background knowledge setting of this study, the occurrence of X14 (Pipe joint seal failure), X23 (Hose fitting rupture), and X25 (weld cracking) need to directly lead to the occurrence of leakage accidents in the HRS and therefore set as the prior knowledge of the model. In analyzing these factors, it is recognized that they are not just single events but may be interrelated and work together to influence the occurrence of leakage accidents. For example, a seal failure in a pipe joint may lead to an increase in pressure, which in turn triggers the rupture of a hose joint. Meanwhile, weld cracks can be caused by prolonged use or improper installation, further increasing the risk of leakage. Similarly, improper fabrication may occur during routine

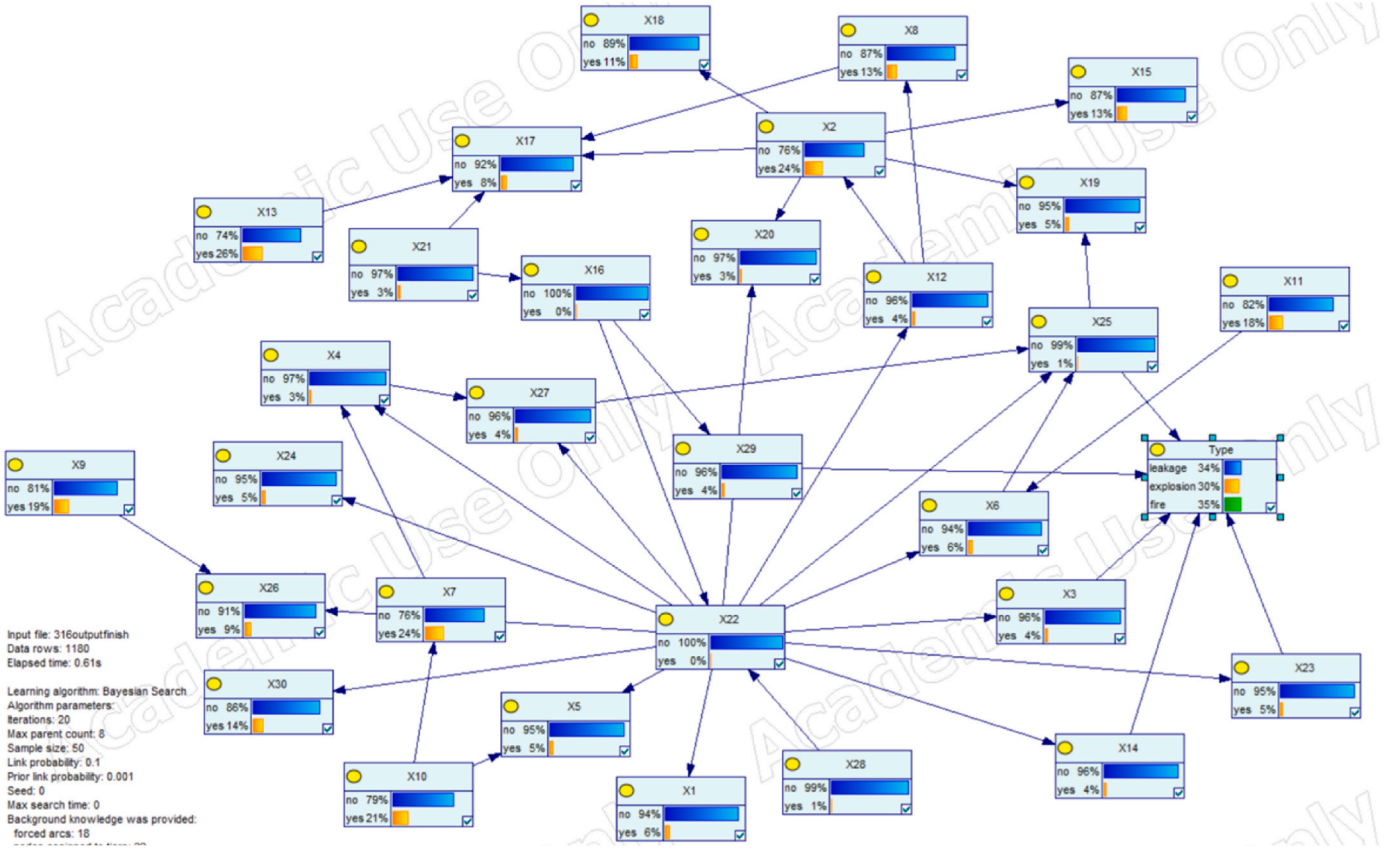

Fig. 9. BN modeling of HRS accidents.

maintenance due to lack of training or experience on the part of personnel. In an emergency, employees without specialized training may make poor decisions that exacerbate the consequences of an accident, leading to a series of failures that are reflected in background knowledge. The combination of these factors provides a more comprehensive view of the model and helps us to better understand the potential safety hazards of HRS.

To better compare the advantages and disadvantages of each model, three different types of structure learning algorithms were selected for systematic analysis and comparison. These three algorithms are constraint-based structure learning (PC), score-based structure learning (BS), and probabilistic and graph theory-based structure learning (GTT). For example, Figs. 6 and 7 show the structure learning results developed by GTT algorithm and PC algorithm, respectively.

4.2. BN parameter learning

Parameter learning is the process of estimating unknown parameters in a model from data given by the model structure. It is concerned with optimizing the parameters of the model so that the model can best describe the data. The methods of BN parameter learning mainly include maximum likelihood estimation (MLE) and the EM algorithm [47]. The EM algorithm is an extension of the MLE and focuses on the case of dealing with hidden variables or missing data, optimizing the parameters step by step by step by means of an iterative process. The MLE does not consider the a prior information, whereas the BN model developed in this paper is complex, with a prior knowledge from the literature as well as from experts. Therefore, although the data in this paper is complete, MLE cannot address the complexities regarding parameterized distributions, and parameter learning using MLE may lead to poor model performance. For complex dependency structures, EM can effectively decompose the problem and simplify the parameter estimation process.

In this section, EM algorithm is utilized to launch the parameter learning of the BN model. The EM algorithm consists of two steps, the E-step and the M-step. First, it computes the expectation of the hidden variables given the current parameters, and then maximizes the expectation computed in the E-step to update the parameters.

In the E-step, the posterior distribution of the hidden variables is computed given the observed data and the current parameters. Using the structure of BN, the expectation of a hidden variable can be computed by methods such as forward-backward algorithms or variational inference. For example, if there is a hidden variable Z and the observed variable is X, the expectation of the logarithmic likelihood function with respect to Z can be computed, as shown in formula (5) [48]:

$$Q(\theta|\theta^{(t)}) = E_{(Z|X,\theta^t)}\, LnP(Z,X|\theta^{(t)}) \tag{5}$$

where $\theta^{(t)}$ is the current parameter. X is the given observation. $Q(\theta|\theta^{(t)})$ refers to the function that computes the expected value of the hidden variable Z under the current parameter $\theta^{(t)}$. $P(Z,X|\theta^{(t)})$ refers to the posterior probability distribution of the hidden variable Z.

In the M-step, the parameters of the BN are updated using the expectation of the hidden variables computed in the E-step. For CPT, the parameters can be updated by maximizing the likelihood function using the current hidden variable expectations, as shown in formula (6) [48]:

$$\theta^{(t+1)} = \underset{\theta}{argmax} Q(\theta|\theta^{(t)}) \tag{6}$$

where $\theta^{(t+1)}$ denotes the updated model parameters in the t+1st iteration.

Convergence judgement is a critical step to ensure stable and effective model training. Monitoring the log-likelihood function (Log-Likelihood) is a common method used to verify the convergence of the EM

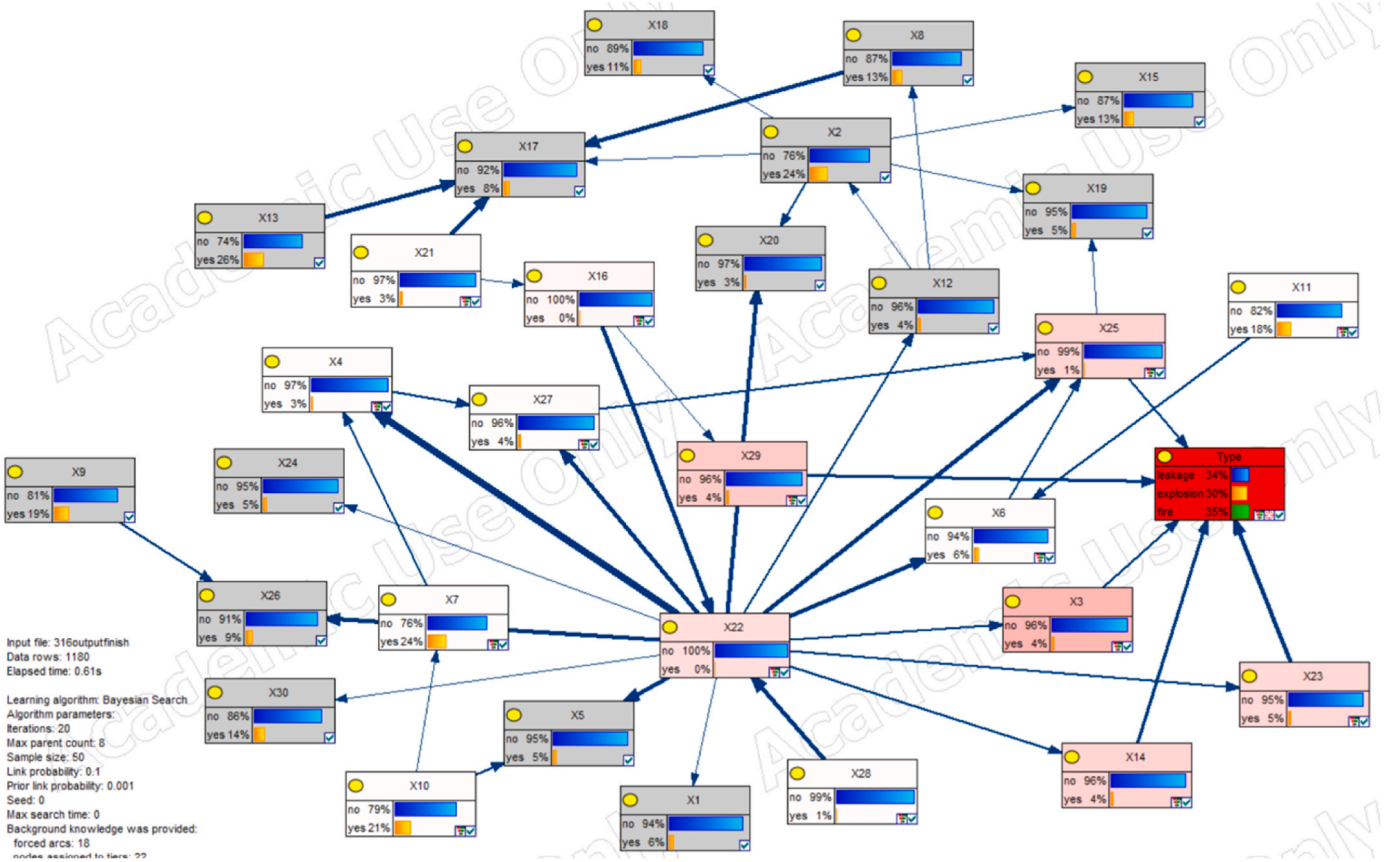

Fig. 10. Sensitivity network for HRS accidents.

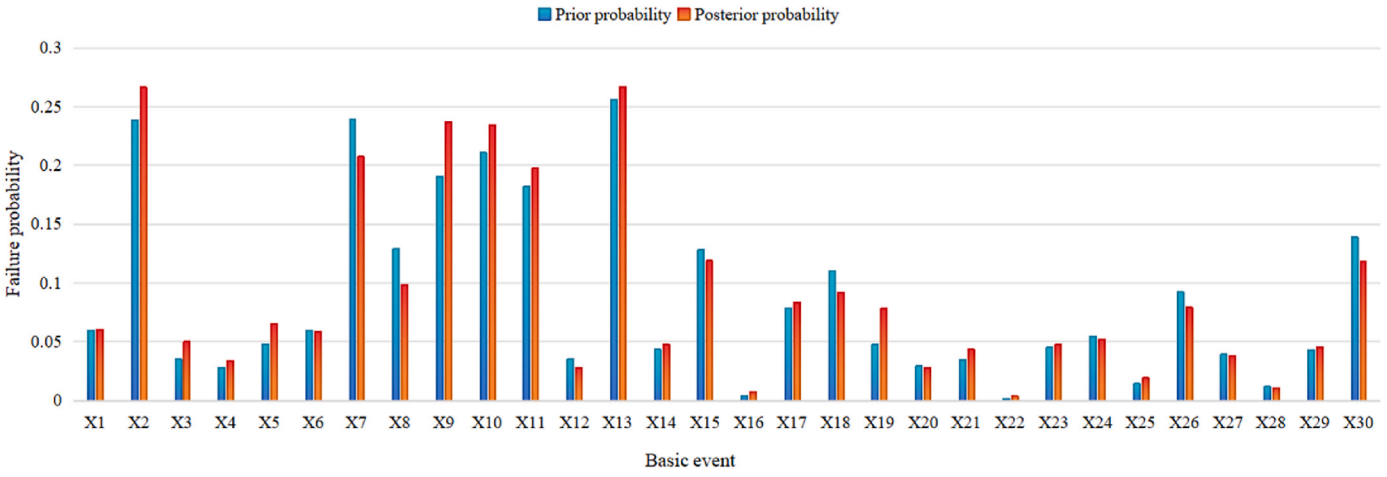

Fig. 11. Comparison of the prior and posterior probability under leakage accident.

algorithm, which is based on the principle of calculating the log-likelihood function $L(\theta)$ in each iteration and recording its value. If the change in the log-likelihood function is less than a set threshold ϵ in successive iterations, the algorithm is considered to have converged [49], as show in formula (7).

$$\left|L\left(\theta^{(t+1)}\right) - L(\theta^{(t)})\right| < \epsilon \tag{7}$$

4.3. Model validation

Model validation aims at evaluating the validity and reliability of the constructed BN model to ensure that the model accurately represents the underlying connections in the data and may provide reliable predictions or inferences. In this case, the most appropriate method for model evaluation is K-fold cross-validation. In machine learning practice, many studies and experiments have shown that cross-validation using k = 10 usually yields better generalization performance. Therefore, it has become a widely accepted standard choice. Fig. 8 is a schematic representation of the four parameters in the confusion matrix.

The outputs of the K-fold cross-validation include Overall Accuracy (OA), Precision, Recall, and F_1 score. These predictive index values can be obtained by calculating the confusion matrix for each node, as show in formula (8)-(11) [49]:

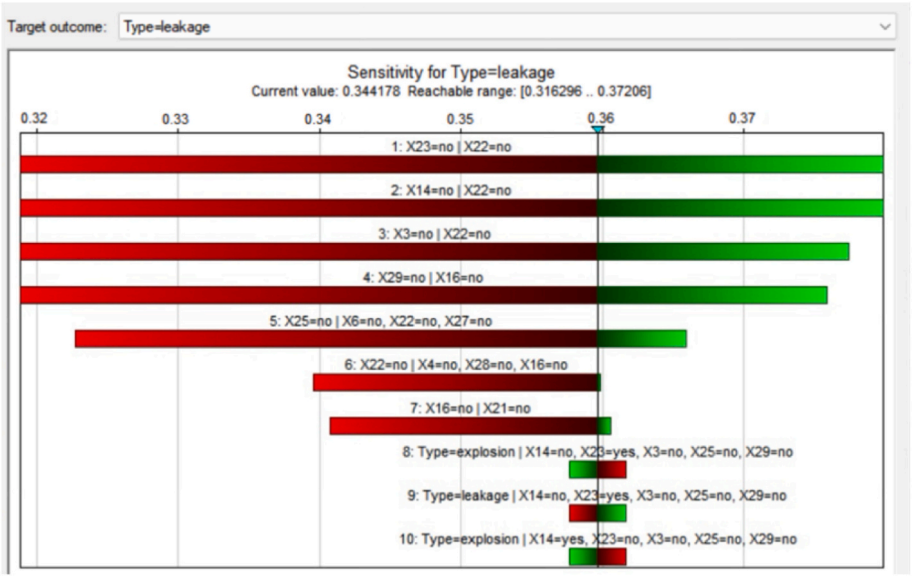

Fig. 12. Sensitivity analysis tornado diagram for leakage state.

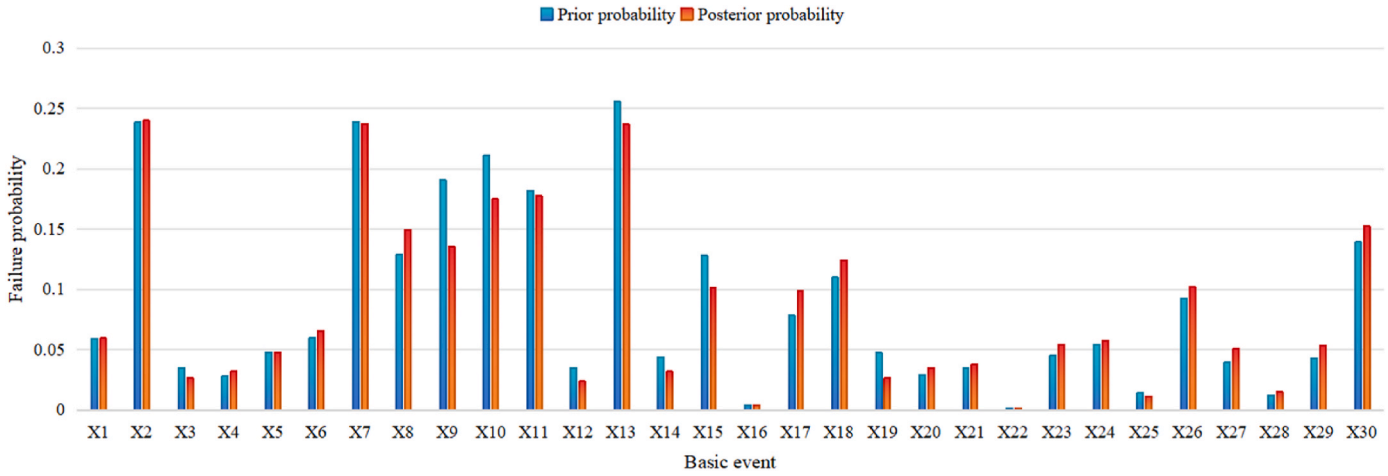

Fig. 13. Comparison of the prior and posterior probability under explosion accident.

$$\text{Overall accuracy} = \frac{T_P + T_N}{T_P + F_P + T_N + F_N} \tag{8}$$

$$\text{Precision} = \frac{T_P}{T_P + F_P} \tag{9}$$

$$\text{Recall} = \frac{T_P}{T_P + F_N} \tag{10}$$

$$\text{F1 score} = 2^{*}\frac{Precision^{*}Recall}{Precision + Recall} \tag{11}$$

We compared the predictive index values of the models generated using BS, GTT and PC, and most of the predictive values in the BS algorithm are greater than those in the GTT algorithm and the PC algorithm, as shown in Table 3. The BS algorithm is lower than the GTT algorithm's predictive value only in the predictive value of prec, which is 0.02%. This shows the good performance of the network structure based on the BS algorithm, and this paper chooses to use the BN model developed by the BS and EM algorithm for the HRS accident study in the next research [50].

Fig. 9 shows the BN model developed by the BS algorithm and EM algorithm.

4.4. Sensitivity analysis

Sensitivity analysis is a technique that can help to understand how input parameters affect output parameters [51], which is an effective means of BN verification. Sensitivity analysis can test the stability, reliability and applicability of the model. We observe the sensitivity of the model to different nodes by perturbing the data to a certain extent. This reveals which factors have a large impact on the model results. A sensitivity analysis was performed to obtain the impact of different factors on the outcome of the three accident types [52].

As shown in Fig. 10, a detailed sensitivity analysis was conducted for the entire BN model. This analysis takes Type as the target node, and the goal is in exploring the degree of influence and importance of other nodes on this target node. The red nodes (X3, X14, X22, X23, X25, X29) are critical to the posterior probability distribution of the target node. These nodes represent the factors that have the greatest impact on the node Type, and any adjustment to these nodes may significantly change the probability values of the target nodes. Therefore, these red nodes need to be prioritized during the optimization of the model to ensure the validity and accuracy of the model. The pink nodes also play an important role in influencing the target nodes, and although their influence is relatively weak. The gray nodes show a very low probability of

influencing the target nodes throughout the analysis [53]. The factors represented by these nodes have almost no significant effect on the posterior probability distribution of Type. Therefore, the adjustment and optimization of these gray nodes can be ranked as the last consideration in the model optimization process to reduce unnecessary complexity and computational cost [54].

The width of the edges in the network indicates the sensitivity of the influence to the target variable, the wider the edge, the greater the influence. There are 40 connecting lines in the model, and there are five connecting lines pointing to the target node, all of which have largest influence on the target node.

The types of accidents in HRS are not only related to the technical condition of the equipment and the skill level of the operators, but also affected by a variety of factors, such as environmental conditions, system design and safety management measures, and different influencing factors need lead to different accidents. Therefore, an in-depth study of the causes of different accident formations is essential to improve the safety of HRS.

4.4.1. Sensitivity analysis of leakage accident

Fig. 11 shows the comparison of the prior probability and posterior probability of different nodes under hydrogen leakage accident. Fig. 12 shows the tornado diagram of the target node (TYPE) when the accident type is set to leakage. The horizontal axis of the bar graph represents the different parameters while the vertical axis represents the range of variation in the state of the target node [55]. The red bar indicates a negative change in the state of the target when the parameter is varied, which means that the change in that parameter needs lead to deterioration in the state of the target node, while the green bar indicates a positive change, which means that the change in the parameter needs lead to improvement in the state of the target node.

Fig. 12 shows the 10 factors that have the greatest impact on the leakage accident. The most significant events affecting the state of the target node in the event of a leakage at the HRS are, in descending order of importance, X23, X14, X3, X29 and X 25. Therefore, corresponding measures can be taken for the above nodes to avoid leakage. For example, regarding X23 and X14, reliable materials can be selected according to the usage or working environment, and old joints can be inspected and replaced regularly to avoid hydrogen leakage. Once high pressure or leakage in the system, install emergency pressure relief valves or venting devices near the fittings to ensure that the gas can be released quickly to avoid rupture of the fittings or serious accidents.

Based on the BN diagnosis results, X23, X14 and X3 are affected by node X22, highlighting the severe effects of an electrical short circuit. Similarly, X29 is affected by X16, reflecting problems with regular maintenance, environmental control, and overload protection [56].

4.4.2. Sensitivity analysis of explosion accident

Similarly, Fig. 13 shows the comparison of the prior probability and posterior probability of different nodes under hydrogen leakage accident. Fig. 14 is a tornado diagram of the full range of sensitivity analysis of the BN model when the explosion accident occurs. It is obvious that under the explosion accident, the most influential ones are X25, X3, X14, X23, X29, and X16. X25 (weld cracking) is the node with the highest sensitivity. Regarding weld cracking, the key lies in choosing suitable materials, optimizing the welding process, strengthening the post-weld treatment, and implementing strict quality control and regular inspection [57]. The high sensitive nodes are affected by different parent nodes in different accident states. X25 is affected by parent node ×5 in the explosion state, X3, X14, X23 by X16 and X14 by X22 at the same time. These problems are caused by the lack of electrical overload protection, good grounding and insulation or lack of operator training. Meanwhile, X5 (insufficient screw torque value) is due to lack of a standardized torque management system or regular inspections, which can be avoided by using measures such as anti-loosening devices in critical areas to avoid insufficient torque values for screws [58].

In addition, compared with the tornado graph in the leakage state, it is found that the nodes that have an impact on the target node remain basically the same. This suggests that these key nodes play similar roles in the network regardless of the different accident states. This stability reflects the intrinsic connection between the nodes and suggests that the influence of specific nodes on the system dynamics is continuous and reliable under multiple states [59].

4.4.3. Sensitivity analysis of fire accident

When the fire accident occurs, the posterior probability of each node is compared with the prior probability, as shown in Fig. 15. Fig. 16 is a tornado diagram of the full range of sensitivity analysis of the BN model when the fire accident is set as the target variable of the sensitivity analysis. Fig. 16 shows the 10 factors that have the greatest impact on the fire accident, in which the most influential is X25.

Sensitivity order from high to low is as follows: X25, X3, X23, X29, X14. The order of these nodes indicates the degree of their impact on the HRS at the time of the fire event. It is noteworthy that this result is

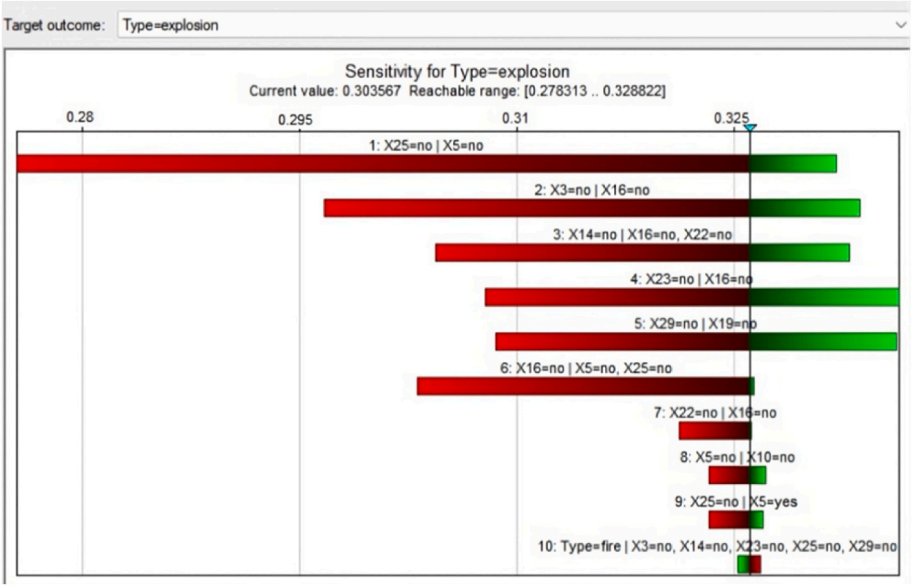

Fig. 14. Tornado diagram for explosion accident.

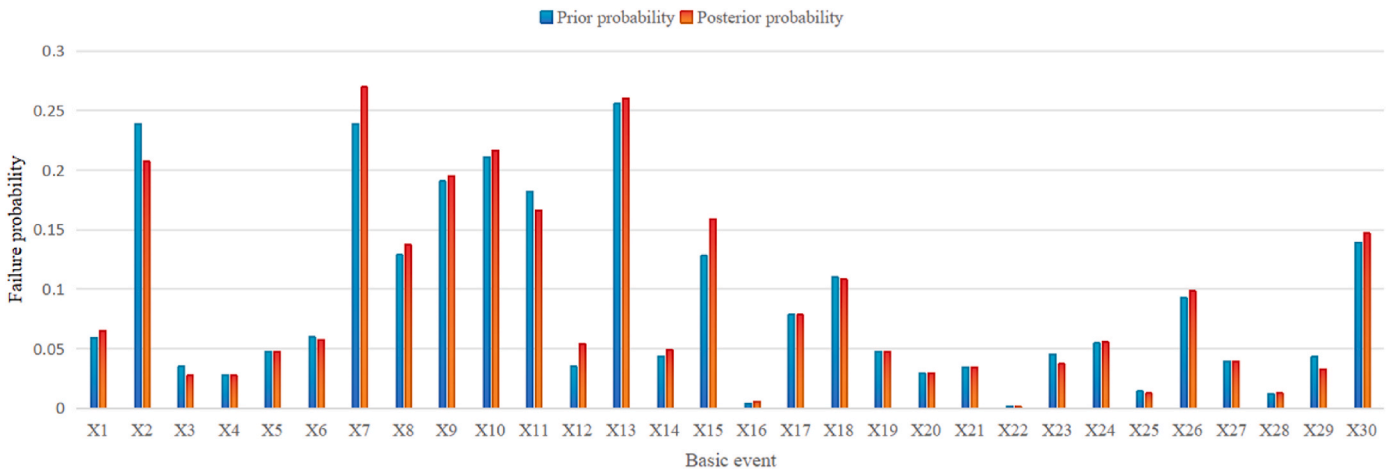

Fig. 15. Comparison of the prior and posterior probabilities of nodes under fire accident.

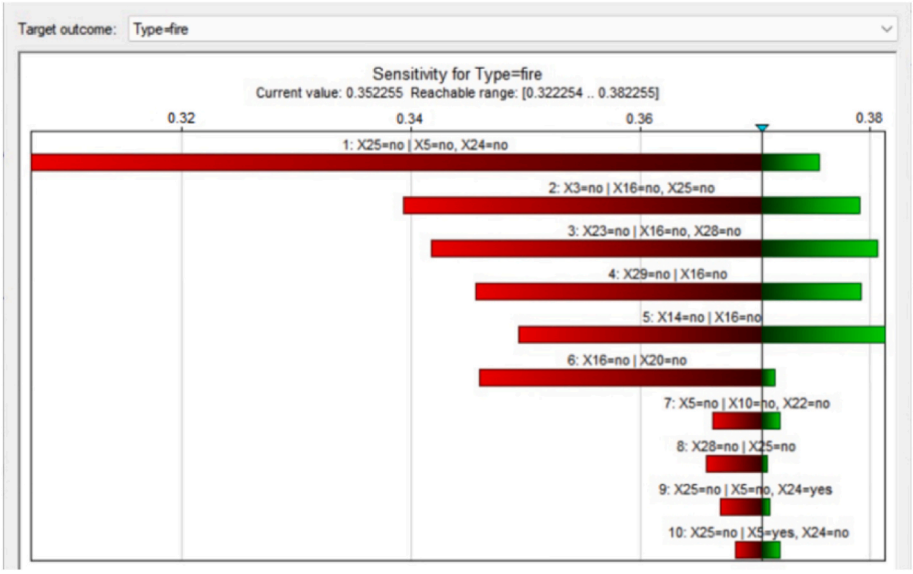

Fig. 16. Sensitivity analysis tornado diagram for fire accident.

generally consistent with previous analyses of leakage and explosion hazards. This consistency suggests that the effects of the main causal factors are similar in hydrogen station-related accidents, despite the different types of accidents. Specifically, the factors X25, X3, X23, X29, X14, and X16 consistently show a strong influence on the occurrence and development of accidents in different hazard scenarios, reflecting their central role in hydrogen station safety management and risk assessment.

5. Conclusion

In this study, a physics-informed data-driven BN for risk analysis of HRS is proposed. 30 RIFs are identified by applying the HAZID accident data and related literatures. To solve the problem of insufficient data, physics information is integrated to define the coercive relationship of BN nodes. Additionally, to improve the precision of the results CTGAN is applied to augment the pre-processing data. Moreover, BS, PC and GTT methods are resorted to conduct BN structuring learning, respectively. By leveraging EM algorithm, three BNs for HRS risk analysis are obtained. Comparing the performance of above three BNs, the BN of HRS risk analysis by BS and EM are selected to conduct sensitivity analysis due to their relative high performance with prediction accuracy is 91.8%. Through the results, we found that the critical node with the greatest impact on leakage accidents is X23, and the critical node with the greatest impact on both explosion and fire accidents is X25. Although the critical node with the greatest impact on these accidents are different, we found that the critical nodes with a greater impact on them are essentially the same in the sensitivity analysis. These critical nodes include X3 (vehicle collision), X14 (pipe joint seal failure), X16 (pressure detection device failure), X23 (hose joint rupture), X25 (weld cracking), and X29 (third party influence). These nodes show high impacts in different accident scenarios, indicating that they are non-negligible factors in the safety management of HRS.

The methodology proposed in this paper can be widely applicated in other industries. For example, in the field of transportation, Zaili Yang et al. used data-driven Bayes to explore the impact of different risk factors on maritime casualties over time, to formulate more reasonable safety measures [60]. Yuhao Cao et al. used the Tree Augmented Network (TAN) to develop a data-driven BN model to analyze the relationship between the severity of maritime accidents and the associated accident influencing factors (AIFs) [61].

The sensitivity analysis in the paper reveals the key factors influencing the occurrence of accidents at hydrogen refueling stations, and this analytical approach is also applicable to other industries. Bakhtiari et al. combined BN and the Strongest Path Method (SPM) to assess the robustness risk in infrastructure systems [62]. In future work, dynamic

risk assessment of HRS is needed to capture the degradation performance of critical components. Meanwhile, the dynamic risk assessment method can help predict the time point of equipment failure and optimize the maintenance strategy to avoid unexpected accidents.

CRediT authorship contribution statement

Jinduo Xing: Writing- Reviewing and Editing, Writing-original draft, Validation, Supervision, Methodology, Investigation, Funding acquisition, Conceptualization; **Jiaqi Qian:** Investigation, Visualization, Writing- Original draft preparation; **Rui Peng:** Reviewing and Editing; **Enrico Zio:** Writing- Reviewing and Editing.

Declaration of competing interest

The authors declare that they have no known competing financial interests or personal relationships that could have appeared to influence the work reported in this paper.

Acknowledgment

The work of Dr. Jinduo Xing is supported by the Fundamental Research Funds for R&D Program of Beijing Municipal Education Commission (Grant No. KM202310016003) and Beijing University of Civil Engineering and Architecture (Grant No. X21056).

Appendix A. Supplementary data

Supplementary data to this article can be found online at https://doi.org/10.1016/j.ijhydene.2025.02.110.

References

[1] Abu Sayem M, Hannan MA, Rahman SA, Long Chua Yaw, Jern Ker Pin, Wong Richard TK, Jang Gilsoo. An effective optimization algorithm for hydrogen fuel cell-based hybrid energy system: a sustainable microgrid approach. Int J Hydrogen Energy 2025;98:1341–55.
[2] Lim Hyun Sung, Kang Byeonghyun, Ahn Minhyeok, Kim Min Soo. Optimizing hydrogen utilization in Fuel Cell Hybrid Vehicles: modeling fuel cell systems and managing energy between batteries and fuel cells. Int J Hydrogen Energy 2025;99:819–35.
[3] Malozyomov BV, Porsev EG. Portable energy sources based on hydrogen fuel cell with regeneration. Int J Hydrogen Energy 2024;93:1179–88.
[4] H2stations.org. Available from: https://www.h2stations.org/; 2024 28 Oct 2024.
[5] Deng Shanshan, Li Feng, Luo Hao, Yang Tianqi, Ye Feng, Chahine Richard, Xiao Jinsheng. Lumped parameter modeling of SAE J2601 hydrogen fueling tests. Sustainability 2023;15. https://doi.org/10.3390/su15021448.
[6] China Battery. Cause of Norwegian hydrogen station explosion identified, giving China's hydrogen industry a piece of mind. Available from: http://www.caam.org.cn/chn/38/cate_430/con_5224848.html; 2019 28 Oct 2024.
[7] Hoseyni Seyed Mojtaba, Mostafa Mohamed Osman Mesbah, Cordiner Joan. Mitigating risks in hydrogen-powered transportation: a comprehensive risk assessment for hydrogen refuelling stations, vehicles, and garages. Int J Hydrogen Energy 2024;91:1025–44.
[8] Odoi-Yorke Flavio, Agyekum Ephraim Bonah, Rashid Farhan Lafta, Davis John Eshun, Hussein Togun. Trends and determinates of hydrogen energy acceptance, or adoption research: a review of two decades of research. Sustain Energy Technol Assess 2025;73:104159.
[9] Hossain Md Shameem, Islam Md Nasirul, Shahriar Khaza, Hasan Mohammad Mujtaba, Sohag Hossain Md. The role of solar thermal hydrogen production technologies in future energy solutions: a review. Energy Convers Manag X 2025;25:100876.
[10] Mobayen Saleh, Assareh Ehsanolah, Izadyar Nima, Jamei Elmira, Ahmadinejad Mehrdad, Ghasemi Amir, Agarwal Saurabh, Pak Wooguil. Multi-functional hybrid energy system for zero-energy residential buildings: integrating hydrogen production and renewable energy solutions. Int J Hydrogen Energy 2025;102:647–72.
[11] Bokde Neeraj Dhanraj. A unified framework for multi-type hydrogen production and storage in renewable energy systems. Energy Convers Manag X 2025;25:100847.
[12] Roozbahani Abbas, Ghanian Tahereh. Risk assessment of inter-basin water transfer plans through integration of Fault Tree Analysis and Bayesian Network modelling approaches. J Environ Manag 2024;356:120703.
[13] Djemai Zahra, Aissani Nassima, Bekrar Abdelghani, Lounis Zoubida. Risk analysis of petroleum storage tank based on uncertain data incorporated into mapped Bow-tie to Bayesian network. Process Saf Environ Prot 2024;190:1202–21.
[14] Luan Tingting, Li Hongru, Wang Kai, Zhang Xue, Li Xiaoyun. Knowledge graph-based Bayesian network risk assessment model for hydrogen accidents. Int J Hydrogen Energy 2024;81:927–41.
[15] Huixing Meng, Xu An, Li Daiwei, Zhao Shijun, Enrico Zio, Liu Xuan. Jinduo Xing. A STAMP-Game model for accident analysis in the oil and gas industry. Petroleum Science 2024;21:2154–67.
[16] Li Yuntao, Lin Yu, Qi Jing. Dynamic risk assessment method for urban hydrogen refueling stations: a novel dynamic Bayesian network incorporating multiple equipment states and accident cascade effects. Int J Hydrogen Energy 2024;54:1367–85.
[17] Xing Yuxuan, Wu Jiansong, Bai Yiping, Cai Jitao, Zhu Xiaoping. All-process risk modelling of typical accidents in urban hydrogen refueling stations. Process Saf Environ Prot 2022;166:414–29.
[18] He Qian, Peng Shiliang, Zhang Zongjie, He Yuxuan, Fan Lin, Yang Zhaoming, Wang Xiao, Shi Xinna, Su Huai, Zhang Jinjun. A systematic framework of resilience assessment based on multi-state transition modeling under two-phase recovery for hydrogen refueling stations. Int J Hydrogen Energy 2024;90:481–97.
[19] Wang Lin, Lyu Xuefeng, Zhang Jiayu, Liu Fang, Li Xiangbin, Qiu Xiaojun, Song Qingyao, Lin Jiancheng, Ma Tie. Analysis of hydrogen leakage behavior and risk mitigation measures in a hydrogen refueling station. Int J Hydrogen Energy 2024;83:545–52.
[20] Li Huanhuan, Ren Xujie, Yang Zaili. Data-driven Bayesian network for risk analysis of global maritime accidents. Reliab Eng Syst Saf 2023:230.
[21] Zhang Xinqi, Shi Jihao, Li Junjie, Huang Xinyan, Fu Xiao, Wang Qiliang, Usmani Asif Sohail, Chen Guoming. Hydrogen jet and diffusion modeling by physics-informed graph neural network. Renewable and Sustainable Energy Reviews 2025;207:114898.
[22] Islam Rafiqul, Shabani Bahman. Prediction of electrical conductivity of TiO2 water and ethylene glycol-based nanofluids for cooling application in low temperature PEM fuel cells. Energy Proc 2019;160:550–7.
[23] Tan Haibo, Ma Benxue, Xu Ying, Dang Fumin, Yu Guowei, Bian Huitao. An innovative variant based on generative adversarial network (GAN): regression GAN combined with hyperspectral imaging to predict pesticide residue content of Hami melon. Spectrochim Acta Mol Biomol Spectrosc 2025;325:125086.
[24] Lu Yuzhen, Chen Dong, Olaniyi Ebenezer, Huang Yanbo. Generative adversarial networks (GANs) for image augmentation in agriculture: a systematic review. Comput Electron Agric 2022;200:107208.
[25] Jiangzhou Deng, Songli Wang, Jianmei Ye, Lianghao Ji, Yong Wang. *DGRM*: diffusion-GAN recommendation model to alleviate the mode collapse problem in sparse environments. Pattern Recogn 2024;155:110692.
[26] Peng Kexin, Iima Hitoshi, Kitamura Yoshihiro. Predicting FX market movements using GAN with limit order event data. Finance Res Lett 2025;72:106527.
[27] He Biao, Jahed Armaghani Danial, Lai Sai Hin, Samui Pijush, Mohamad Edy Tonnizam. Applying data augmentation technique on blast-induced overbreak prediction: resolving the problem of data shortage and data imbalance. Expert Syst Appl 2024;237:121616.
[28] Zhang Kang, Zhong Guoqiang, Dong Junyu, Wang Shengke, Wang Yong. Stock market prediction based on generative adversarial network. Procedia Comput Sci 2019;147:400–6.
[29] Wang You, Fan Qianjun, Dai Fang, Wang Rui, Ding Bosong. A physics-data-driven method for predicting surface and building settlement induced by tunnel construction. Comput Geotech 2025;179:107020.
[30] Li Qin, Zhang Boyuan, He Hongwen, Wang Yong, He Deqiang, Mo Shuai. A hybrid physics-data driven approach for vehicle dynamics state estimation. Mech Syst Signal Process 2025;225:112249.
[31] Meng Huixing, An Xu, Xing Jinduo. A data-driven Bayesian network model integrating physical knowledge for prioritization of risk influencing factors. Process Saf Environ Prot 2022;160:434–49.
[32] Meng Huixing, Hu Mengqian, Kong Ziyan, Niu Yiming, Liang Jiali, Nie Zhenyu, Xing Jinduo. Risk analysis of lithium-ion battery accidents based on physics-informed data-driven Bayesian networks. Reliability Engineering and System Safety 2024;251:110294.
[33] Glück Tobias, Lobe Amadeus, Trachte Adrian, Bitzer Matthias, Kemmetmüller Wolfgang. Hybrid control of hydraulic directional valves: integrating physics-based and data-driven models for enhanced accuracy and efficiency. ISA (Instrum Soc Am) Trans 2024.
[34] Wang Jian, Gao Shibin, Yu Long, Ma Chaoqun, Zhang Dongkai, Kou Lei. A data-driven integrated framework for predictive probabilistic risk analytics of overhead contact lines based on dynamic Bayesian network. Reliab Eng Syst Saf 2023;235:109266.
[35] Liu Kezhong, Yu Qing, Yang Zhisen, Wan Chengpeng, Yang Zaili. BN-based port state control inspection for Paris MoU: new risk factors and probability training using big data. Reliab Eng Syst Saf 2022:224.
[36] Tools Hydrogen. Hiad - hydrogen incident and accident database. Available from: https://h2tools.org/bibliography/hiad-hydrogen-incident-and-accident-database; 2024 28 Oct 2014.
[37] Sun Xuting, Hu Yue, Qin Yichen, Zhang Yuan. Risk assessment of unmanned aerial vehicle accidents based on data-driven Bayesian networks. Reliab Eng Syst Saf 2024;248:110185.
[38] Lin YH, Li GH. Uncertainty-aware fault diagnosis under calibration. IEEE Trans Syst Man Cybernet: Systems 2024;54(10):6469–81.
[39] Yoo Jeong Do, Kim Haerin, Kim Huy Kang. GUIDE: GAN-based UAV IDS enhancement. Comput Secur 2024;147:104073.
[40] Ouidadi Hasnaa, Guo Shenghan. MPS-GAN: a multi-conditional generative adversarial network for simulating input parameters' impact on manufacturing processes. J Manuf Process 2024;131:1030–45.

[41] Mucllari Edison, Cao Yue, Ye Qiang, Zhang YuMing. Modeling imaged welding process dynamic behaviors using Generative Adversarial Network (GAN) for a new foundation to monitor weld penetration using deep learning. J Manuf Process 2024;124:187–95.
[42] Li Junhao, He Junjiang, Li Wenshan, Fang Wenbo, Yang Geying, Li Tao. SynDroid: an adaptive enhanced Android malware classification method based on CTGAN-SVM. Comput Secur 2024;137:103604.
[43] Tang Daogui, Zheng Zihuan, Guerrero Josep M. A hybrid multi-criteria dynamic sustainability assessment framework for integrated multi-energy systems incorporating hydrogen at ports. Int J Hydrogen Energy 2025;99:540–52.
[44] Seo Jangwon, Hwang Hyo-Seok, Lee Minhyeok, Seok Junhee. Stabilized GAN models training with kernel-histogram transformation and probability mass function distance. Appl Soft Comput 2024;164:112003.
[45] Anidjar Or Haim, Marbel Revital, Dubin Ran, Dvir Amit, Chen Hajaj. Extending limited datasets with GAN-like self-supervision for SMS spam detection. Comput Secur 2024;145:103998.
[46] Wang Songbo, Stratford Tim, Li Yang, Li Biao. Data-driven estimates of the strength and failure modes of CFRP-steel bonded joints by implementing the CTGAN method. Eng Fract Mech 2024;299:109962.
[47] Meng Huixing, Hu Mengqian, Kong Ziyan, Niu Yiming, Liang Jiali, Nie Zhenyu, Xing Jinduo. Risk analysis of lithium-ion battery accidents based on physics-informed data-driven Bayesian networks. Reliab Eng Syst Saf 2024;251:110294.
[48] Wu Bing, Tang Yuheng, Yan Xinping, Soares Carlos Guedes. Bayesian Network modelling for safety management of electric vehicles transported in RoPax ships. Reliab Eng Syst Saf 2021;209:107466.
[49] Li Huanhuan, Ren Xujie, Yang Zaili. Data-driven Bayesian network for risk analysis of global maritime accidents. Reliab Eng Syst Saf 2023;230:108938.
[50] Liu Jiongjiong, Zhang Jinfen, Yang Zaili, Wan Chengpeng, Zhang Mingyang. A novel data-driven method of ship collision risk evolution evaluation during real encounter situations. Reliab Eng Syst Saf 2024;249:110228.
[51] Liu Keyang, Cai Baoping, Wu Qibing, Chen Mingxin, Yang Chao, Khan Javed Akbar, Wang Chenyushu, Pattiyakumbura Hasini Vidumini Weerawarna, Ge Weifeng, Liu Yonghong. Risk identification and assessment methods of offshore platform equipment and operations. Process Saf Environ Prot 2023;177:1415–30.
[52] Zhang Jun, Yin XiaoLiang, Xing Jinduo, An Xu. Dynamic risk assessment for train brake system considering time-dependent components and human factors. Comput Ind Eng 2023;185:109687.
[53] Li Pengchang, Wang Yuhong, Yang Zaili. Risk assessment of maritime autonomous surface ships collisions using an FTA-FBN model. Ocean Eng 2024;309:118444.
[54] Li Huanhuan, Zhou Kaiwen, Zhang Chao, Bashir Musa, Yang Zaili. Dynamic evolution of maritime accidents: comparative analysis through data-driven Bayesian Networks. Ocean Eng 2024;303:117736.
[55] Qin Chuan, Tian Ying, Yang Zirong, Dong Hao, Feng Lili. Quantitative analysis of hydrogen leakage flow measurement and calculation in the on-board hydrogen system pipelines. Int J Hydrogen Energy 2024;89:1025–39.
[56] Zhou Chilou, Yang Zhen, Chen Guohua, Xiang Li. Optimizing hydrogen refueling station layout based on consequences of leakage and explosion accidents. Int J Hydrogen Energy 2024;54:817–36.
[57] He Xu, Kong Depeng, Yang Guodong, Yu Xirui, Wang Gongquan, Peng Rongqi, Zhang Yue, Dai Xinyi. Hybrid neural network-based surrogate model for fast prediction of hydrogen leak consequences in hydrogen refueling station. Int J Hydrogen Energy 2024;59:187–98.
[58] Alfasfos Rami, Sillman Jani, Soukka Risto. Lessons learned and recommendations from analysis of hydrogen incidents and accidents to support risk assessment for the hydrogen economy. Int J Hydrogen Energy 2024;60:1203–14.
[59] Truong Tam T, Airao Jay, Hojati Faramarz, Ilvig Charlotte F, Azarhoushang Bahman, Karras Panagiotis, Aghababaei Ramin. Data-driven prediction of tool wear using Bayesian regularized artificial neural networks. Measurement 2024;238:115303.
[60] Fan Shiqi, Yang Zaili. Towards objective human performance measurement for maritime safety: a new psychophysiological data-driven machine learning method. Reliab Eng Syst Saf 2023;233:109103.
[61] Cao Yuhao, Wang Xinjian, Wang Yihang, Fan Shiqi, Wang Huanxin, Yang Zaili, Liu Zhengjiang, Wang Jin, Shi Runjie. Analysis of factors affecting the severity of marine accidents using a data-driven Bayesian network. Ocean Eng 2023;269:113563.
[62] Bakhtiari Soheil, Reza Najafi Mohammad, Goda Katsuichiro, Peerhossaini Hassan. Integrated Bayesian Network and Strongest Path Method (BN-SPM) for effective multi-hazard risk assessment of interconnected infrastructure systems. Sustain Cities Soc 2024;104:105294.